

# Capacity assessment of existing corroded overhead power line structures subjected to synoptic winds

Huawei Niu<sup>1</sup>, Xuan Li<sup>2</sup> and Wei Zhang<sup>\*2</sup>

<sup>1</sup>Wind Engineering Research Center, Hunan University, Changsha, China

<sup>2</sup>Department of Civil and Environmental Engineering, University of Connecticut, Storrs, Connecticut 06269, USA

(Received October 12, 2017, Revised April 26, 2018, Accepted May 2, 2018)

**Abstract.** The physical infrastructure of the power systems, including the high-voltage transmission towers and lines as well as the poles and wires for power distribution at a lower voltage level, is critical for the resilience of the community since the failures or nonfunctioning of these structures could introduce large area power outages under the extreme weather events. In the current engineering practices, single circuit lattice steel towers linked by transmission lines are widely used to form power transmission systems. After years of service and continues interactions with natural and built environment, progressive damages accumulate at various structural details and could gradually change the structural performance. This study is to evaluate the typical existing transmission tower-line system subjected to synoptic winds (atmospheric boundary layer winds). Effects from the possible corrosion penetration on the structural members of the transmission towers and the aerodynamic damping force on the conductors are evaluated. However, corrosion in connections is not included. Meanwhile, corrosion on the structural members is assumed to be evenly distributed. Wind loads are calculated based on the codes used for synoptic winds and the wind tunnel experiments were carried out to obtain the drag coefficients for different panels of the transmission towers as well as for the transmission lines. Sensitivity analysis is carried out based upon the incremental dynamic analysis (IDA) to evaluate the structural capacity of the transmission tower-line system for different corrosion and loading conditions. Meanwhile, extreme value analysis is also performed to further estimate the short-term extreme response of the transmission tower-line system.

**Keywords:** transmission tower-line system; wind tunnel experiments; dynamic analysis; capacity curves; extreme value analysis

## 1. Introduction

Serving as one key component of the lifeline infrastructure system, overhead power line is usually used for electric power transmission and distribution to transmit electrical energy along long distances (Zhang *et al.* 2015, Yuan *et al.* 2017). It consists of one or more conductors suspended by towers or poles. Overhead power line, especially for transmission towers and lines, could cross over remote regions that are off major transportation networks, which make it difficult for monitoring structural performances and condition assessments. Multiple threats from natural and manmade hazards, such as strong winds for the transmission towers and lines in the mountainous area or valleys, could bring safety concerns of the overhead power line especially after years of operation for these structures. Possible failures from the transmission towers or lines could bring large area blackouts with a further cascading effect that pose severe threats to the regional or national power system security with significant economic loss. This has been a great challenge for the stakeholders, decision makers, and the entire society. In the Americas, Australia, and South Africa, about 80% of the transmission tower failures are due to the strong wind loadings from

tornados, hurricanes, or isolated thunderstorms and such failures could lead to large area power outages (De Oliveira *et al.* 2006). For example, over five million people in the U.S. West Coast lost power on December 22, 1982 after high winds knocked over a major 500-kV transmission tower, which fell into a parallel 500-kV line tower. The failure mechanically cascaded and caused three additional towers to fail on each line (Jacobs 2013). More recently, strong winds and associated tree falling and wire breakage in extreme weather conditions were still reported as a reason for the large area blackout, such as the blackout during Hurricane Sandy in October 2012 for 8.2 million people in 17 states, the District of Columbia and Canada and the blackout during June 2012 Derecho for 4.2 million people in 11 Midwest and Mid-Atlantic states and the District of Columbia.

For individual transmission towers and lines, the site-specific terrains and ambient environments could lead to different local built environment, such as wind environment and soil conditions, etc. Therefore, the wind time histories and the associated wind induced loadings on the transmission tower-line system could be significantly different for the transmission towers even though they are in the same circuit or they have the same structural types. Codes and specifications provide a simplified method to calculate the equivalent static load. However, dynamic responses of the transmission tower-line system could be different. With varied climate conditions, more extreme weather events with stronger wind speeds and higher

---

\*Corresponding author, Assistant Professor  
E-mail: [wzhang@enr.uconn.edu](mailto:wzhang@enr.uconn.edu)

frequencies could lead to more safety concerns of the overhead power infrastructures (Meehl *et al.* 2000). Nevertheless, continuous interactions from the built environment and the structures, corrosion could gradually develop at various locations of the structures. Progressive failure mode of the transmission towers as well as the structural capacity, therefore, could also shift or change accordingly.

In the last decades, extensive studies were performed to investigate the dynamic response of the transmission tower-line system subjected to synoptic winds and non-synoptic winds either experimentally or numerically. Lin *et al.* (2012) conducted a series of experiments to study the responses of an aeroelastic model of transmission lines and support structures under two types of wind, i.e., boundary layer wind and downburst wind. Later on, boundary layer wind tunnel tests were conducted by Liang *et al.* (2015) to investigate dynamic responses of the transmission tower with and without lines under various wind speeds. The effect of coupling between towers and lines as well as the cross-wind vibration of the tower were assessed for designing a wind resistant transmission tower-line system. To simplify the calculation procedure for the reactions of transmission lines subjected to downburst loads, an approximate closed form solution was proposed by Aboshosha and El Damatty (2015) and the results showed a good agreement with those from the finite element analysis. Focusing on the effect of downburst wind on the transmission tower-line system, Elawady and El Damatty (2016) performed a nonlinear structural analysis to estimate the longitudinal forces acting on the tower cross arms resulting from the difference in tension forces of the conductors attached to the tower. Darwish and El Damatty (2017) developed a practical simplified load that can represent critical downburst configurations causing transmission towers to fail, followed with a detailed procedure for designing transmission towers under downburst loads. Meanwhile, Yang and Hong (2016) used a finite element model to evaluate the nonlinear response of a transmission tower-line system under downburst wind. They also compared the capacity curves of this system with those of a single tower to identify the effect of dynamic interactions between the tower and the conductors. Elawady *et al.* (2017) experimentally assessed the dynamic response of a multi-span transmission line subjected to downburst winds in terms of the dynamic response factor calculated from their proposed decomposition approach. To investigate the effect of boundary layer winds on the tower-line system, Deng *et al.* (2016) evaluated the dynamic response of a lattice suspension tower-line system under skew incident winds via both experimental and numerical approaches. The effect of the aerodynamic damping on the structural response was also investigated in their study. A review of the previously conducted work related to dynamic responses of a transmission tower-line system under both synoptic and non-synoptic wind loads was made by Aboshosha *et al.* (2016). In their studies, limitations and gaps in the current design codes were identified and suggestions were made for options on filling the research gaps. To further evaluate the aeroelastic characteristics and

structural response of a guyed transmission line system subjected to boundary layer winds, boundary layer wind tunnel tests are conducted under different wind speeds and wind directions by Hamada *et al.* (2017). Their study showed that the transmission line system responded in a quasi-static manner to boundary layer wind loads and the resonant dynamic response component become less significant as wind speed increased.

In this study, to better assess the existing corroded transmission tower and line system, the dynamic performance of the existing transmission tower-line system considering corrosion penetration on structural members and aerodynamic damping force under different wind environmental conditions are evaluated. The paper is organized as the following. After the brief introduction, the incremental dynamic analysis (IDA) is introduced in section 2. In section 3, modeling scheme of the transmission tower-line system is introduced. Wind tunnel tests and wind loading simulations are introduced in section 3, as well. The dynamic responses, capacity curves, and extreme value analysis at different wind yaw angles and wind speeds are presented in Section 4. Finally, section 5 provides some concluding remarks and discussions.

## 2. Structural dynamic analysis

### 2.1 Structural analysis

In the current codes, such as ASCE-74, the wind loads, defined in an orthogonal approach, are modelled in the transverse and longitudinal directions for the design of a transmission tower. With a significant difference of drag loads in different wind directions, the wind loads could be significantly different with that defined in the codes (Mara 2013). In addition, the drag coefficient of the lattice frames is based on the solidity ratio in the design codes. To better understand wind-structure interactions, wind tunnel tests are carried out to get the drag coefficient of the tower and the cable for static wind load. In addition, gust response factor (GSF) can be used to consider dynamic effects.

In the time domain, incremental dynamic analysis, which is originally applied in the field of earthquake engineering, incremental dynamic analysis (IDA) can also be used to evaluate structural performance of the transmission tower-line system under strong lateral wind loads (Banik *et al.* 2008, 2010, Mara 2013). Similar to the concept of scaling seismic loading from ground motions, IDA for wind dynamic analysis also gradually scales up the wind speed and the wind loading to observe the structural linear/nonlinear behavior and identify the structural failure mode. Wind time histories are used for the dynamic analysis to obtain the relationship of loading (such as base shear force) and displacements (such as tower top tip) curves. Damage measures (DM) and their threshold values are usually defined to ensure the safety level of the structure to avoid potential catastrophic failures or nonfunctioning conditions. Since the transmission tower is not central symmetrical and the transmission lines also have their orientations, the structure capacity for the transmission

towers at different wind yaw angles could also be different. Correspondingly, the capacity curves in these wind yaw angles will also be different from the two predefined transverse and longitudinal directions in the design code for the transmission towers. For the natural and built environment around the tower, the dominant wind direction and wind speed will be site specific. The capacity for the transmission tower/lines could also be different.

## 2.2 Modeling of deterioration

For existing structures including the transmission towers, corrosion could grow gradually depending on many parameters for the local built environment (e.g., humidity level, precipitations, temperature, chemical contents level etc.). To consider the deterioration especially for steel structures used for civil infrastructures, such as bridges or steel towers, many corrosion models were proposed and the major parameters include the deterioration rate (annual loss) and pattern (roughening and pitting), and fatigue strength reduction (Nowak and Szerszen 2001). For example, an exponential function was typically used to predict the corrosion loss for unprotected metal materials (Komp 1987)

$$R = C_A t^{C_B} \quad (1)$$

where  $R$  represents the average corrosion penetration depth, in  $\mu\text{m}$ ;  $t$  is the number of years; and  $C_A$  and  $C_B$  are the parameters obtained through experimental data analysis. Three deterioration rates (high, medium and low) are defined for the marine, urban, and rural environment (Albrecht and Naemi 1984, Nowak and Thoft-Christensen 2000). The corrosion parameters  $C_A$  and  $C_B$  are assumed to follow the lognormal distribution and their statistical descriptors for different types of environment and materials are listed in the literature (Albrecht and Naemi 1984).

After the protective paints are applied, these paints could be effective in the first 5-15 years depending on the local environmental and operational conditions. Without field measurement or observations, the corrosion rate for the first 5-15 years, therefore, are assumed to be zero for many researchers (Czarnecki and Nowak 2008, Park and Nowak 1997). Therefore, the relationship between the corrosion penetration depth and time, therefore, can be updated accordingly, as shown in Eqs. (2) and (3)

For the first  $t_{ci}$  years of exposure

$$R = 0.0 \quad (2)$$

Beyond the first  $t_{ci}$  years of exposure

$$R = C_A (t - t_{ci})^{C_B} \quad (3)$$

where  $t_{ci}$  represents the corrosion initiation time.

Meanwhile, maintenance schemes are usually applied for these steel structures by the owners. Regular repainting or surface treatment could be applied to increase the service life or maintain the normal service life of the existing structures. With consideration of maintenance schemes in the corrosive environments, such as repainting surfaces, a modified corrosion propagation model was introduced to include the influence of the periodic repainting on the

corrosion loss (Lee *et al.* 2006), as shown in Eqs. (4) and (5)

For  $(i) \cdot t_{rep} + t_{ci} < t \leq (i+1) \cdot t_{rep}$

$$R_i(t) = C_A \cdot (t - i \cdot t_{rep} - t_{ci})^{C_B} \quad (4)$$

Otherwise

$$R_i(t) = R_{i-1}(i \cdot t_{rep}) \quad (5)$$

where  $R_i(t)$  represents the average corrosion penetration in  $\mu\text{m}$  at time  $t$  years during the  $i^{\text{th}}$  repainting period;  $t_{ci}$  represents the corrosion initiation time; and  $t_{rep}$  represents the periodic repainting interval.

In the present study, for a demonstration purpose, the transmission towers are assumed to be located in a marine environment for a 5-year corrosion initiation period in order to evaluate the performance of the transmission towers. Therefore, a high deterioration rate is used and the corrosion parameters  $C_A$  and  $C_B$  can be calculated as 149.8 and 0.755, respectively (Albrecht and Naemi 1984). With a further corrosion development, two additional corrosion scenarios of the transmission towers corresponding to 15 years and 25 years of corrosion are simulated, as well, in order to evaluate corrosion effect of the structures on the dynamic performance of the transmission tower-line system. As a first step, the average corrosion penetration calculated based on the above parameters is applied at all the outer surfaces of the L-shaped and T-shaped steels that compose the transmission towers. It is noteworthy that, in practice, the corrosion penetrations could vary for different members of the structure. Some critical positions such as the joints and the tower legs could experience more corrosion damages. With recent advances in UAV based structural condition assessment, more data from field observations as well as statistical data analysis and pattern analysis on corrosion conditions of the transmission towers will be helpful to refine and update the finite element model. In the present study, the implemented corrosion penetration pattern is for a demonstration purpose and the sensitivity analysis is to help understand how the corrosion might affect the dynamic response of the transmission tower-line system under wind loadings. With the conclusion of the present study, further data analysis and refined finite element modeling and updating could be justified and carried out to move beyond.

## 3. Modeling of structures and loads

### 3.1 Finite element modeling

The transmission tower-line system is modeled in ANSYS as three same single circuit lattice steel towers being connected by three four-bundled conductors of four spans. The prototype of the transmission tower-line system is shown in Fig. 1. The 550-kV transmission tower is 68.6 m high and the side length of the square base is 14.094 m. The structural components of the tower are built with steel angle sections of a 210 GPa elastic modulus. The nonlinear

behavior of the tower is modeled by considering both the material nonlinearity and the geometric nonlinearity. More specifically, the material nonlinearity of the tower members is considered using an ideal bilinear elastoplastic model with 235 MPa yield strength and a small tangent modulus defined as 2% of the initial elastic modulus after yielding. The geometric nonlinearity is included in the large deformation analysis. The details of the finite element model for the transmission tower could be found in the literature (Zhang *et al.* 2015).

The distance between the adjacent towers is 450 m and the conductor sag is 18 m based on the catenary equation. Because the two ground lines on the top have very small diameters compared with the conductors, the wind drag forces are neglected and the two ground lines are not modeled in the structural model. Detailed properties of a single cable among the four-bundled conductor are listed in Table 1. In the transmission tower-line model, the conductors are connected to the transmission towers using suspension type insulator strings. The insulator string is composed of 34 insulators each with the mass of 13 kg and the equivalent characteristic parameters of the insulator string used in the numerical model are listed in Table 2. The finite element model built in the commercial software ANSYS uses 3D beam element with a total of 2,221 elements and 878 nodes for each transmission tower and tension-only link element with the length of 5 m for the conductors and 0.195 m for the insulator strings. The beam elements are rigidly connected to represent the multi-bolted moment resisting connections between tower elements. The four nodes of each transmission tower at the ground level are fixed and the leftmost and rightmost endpoints of the conductors are also fixed. A modal analysis is first carried out for the tower model in ANSYS. The results show that the first mode is lateral vibration with a frequency of 1.592 Hz and the second mode is longitudinal vibration with a frequency of 1.651 Hz. Meanwhile, both of fixed and hinge connection for the tower base are tested in the preliminary study to check their potential effects on the structural performance. For the two types of models, the differences for their first and second natural frequencies are less than 0.5%. For a demonstration purpose, fixed base, which is typically used in many studies (Mara and Hong 2013, Yang and Hong 2016, Zhang *et al.* 2015), is used in the present finite element model.

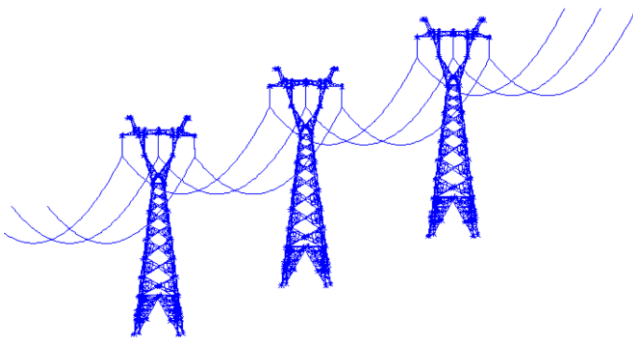


Fig. 1 Model of the transmission tower-line system

Table 1 Conductor properties

Item	Value
Transmission line type	JL/G1A-630/45 Aluminum conductor steel reinforced
Cross-section area (mm <sup>2</sup> )	673.6
Outside diameter (mm)	33.8
Elastic modulus (GPa)	63
Mass per unit length (kg/m)	2.0792
Calculated tensile force (kN)	150450

Table 2 Insulator string parameters

Item	Value
Cross-section area (m <sup>2</sup> )	0.07065
Density (kg/m <sup>3</sup> )	920
Elastic modulus (GPa)	280
Poisson ratio	0.28
Initial force (kN)	36.7

### 3.2 Modeling of wind loads

In the present study, the mean wind speed is calculated based on the power law. The fluctuating wind speed is assumed to be a Gaussian stochastic process and the spectral representation method is used to generate the fluctuating component of wind speed based on spectral density functions (Deodatis 1996). The Kaimal's spectrum (Kaimal *et al.* 1972) is implemented to simulate the longitudinal and lateral fluctuating wind speed, and the Lumley-Panofsky's spectrum is used for simulating the vertical fluctuating wind speed.

Based on the wind speed, the wind drag forces on the conductors can be obtained as

$$F_c = 0.5\rho V^2 \sin^2 \beta C_{dc} dL \quad (6)$$

where  $F_c$  is the total wind loading on the conductor;  $\rho$  is the density of air;  $V$  is the total wind velocity at the height of the conductors consisting of the mean wind speed and the fluctuating component of the wind speed;  $\beta$  is the wind yaw angle between the wind direction and the conductors;  $C_{dc}$  is the drag coefficient for the four-bundled conductor obtained through wind tunnel experiments;  $d$  is the diameter of a single cable; and  $L$  is the span length of the conductors. The wind loads will be applied on the nodes of the tower structural members and the wind load modeling details can be found (Zhang *et al.* 2015).

### 3.3 Modeling of aerodynamic damping

With a long span of the transmission lines and associated slenderness, aerodynamic damping might play an important role in the dynamic response of the entire transmission tower-line system. Recently, many different methods were proposed to model the aerodynamic damping force acted on the long span transmission lines. Dua *et al.* (2015) (Dua *et al.* 2015) and Keyhan *et al.* (2013) introduced an equivalent viscous material damping to represent the influence of the aerodynamic damping on the

cable response in addition to the commonly used structural damping. This method is very easy to implement and requires little modifications to the existed numerical models. However, the suggested value of the equivalent damping ratio is very sensitive to the incident wind speed and direction. To better model the aerodynamic damping, Stengel and Mehdiانpour (2014) and Takeuchi *et al.* (2010) took into account the motion of the transmission lines by using the relative velocity between the wind and the moving conductors. This method possesses quite a good accuracy but requires high computational cost in a transient analysis for extracting the velocity at all nodes of the cables to calculate the wind drag forces at each time step. Chen (2013) proposed an aerodynamic damping model for a stochastic response analysis using a nonlinear function of the time-varying displacement or velocity of vibrations, which was validated by a forced-vibration test in the wind tunnel by comparing the crosswind response. However, this method is based on modal analysis and will be very complicated for a complex transmission tower-line system with numerous degrees of freedom. In the present study, considering the computational cost and the applicability of the methods mentioned above, the method from Stengel and Mehdiانpour (2014) and Takeuchi *et al.* (2010) is adopted to investigate the effect of aerodynamic damping on the dynamic response of the entire transmission tower-line system.

Three groups of simulations are conducted by applying the aerodynamic damping force on the conductors, including the non-corrosive situation of the transmission tower and another two situations of the transmission tower with different corrosion conditions. The wind drag forces on the conductors considering the effect of aerodynamic damping are then calculated as

$$F_c = 0.5\rho(V \sin \beta - u)^2 C_{dc} dL \quad (7)$$

where  $u$  is the velocity of the conductors and the interpretations of other parameters are same as those defined in Eq. (6).

### 3.4 Drag coefficients of towers

The drag coefficients for the transmission tower were obtained through wind tunnel experiments. The wind tunnel experiments for the transmission tower model were carried out in HD-2 wind tunnel at Hunan University, China. The test section of the wind tunnel is 2.5 m high, 3.0 m wide and 17.0 m long. Considering both the size limitation of the wind tunnel and the fabrication accuracy of the transmission tower model, a rigid model with 1/40 scale is used to achieve a better measurement of the drag coefficients. The rigid model in the wind tunnel is shown in Fig. 2. Detailed information about the experimental measuring procedures and the tested drag coefficients for each subsection in different wind directions can be found in (Zhang *et al.* 2015). For a demonstration purpose, only four wind yaw angles of 0°, 30°, 60° and 90° are taken into account in the present study.



Fig. 2 Rigid tower model in wind tunnel



Fig. 3 Conductor model in wind tunnel

### 3.5 Drag coefficients of conductors

In the transmission tower-line system, the four-bundled ACSR (aluminum conductor steel reinforced) conductors with a distance of 400 mm between adjacent cables are used, which are supported by insulator strings on the transmission towers. The characteristic parameters of the four-bundled conductors can be found in Table 1. To measure the drag coefficients for the conductor, wind tunnel experiments are also carried out for the real conductor as shown in Fig. 3. The four-bundled conductor model is connected to a six-component force balance on a turntable and the drag coefficients are tested in the smooth flow. Considering the Reynold number effect and wind attack angle, two wind speeds are chosen to measure the drag coefficients for the four-bundled conductor model at different wind attack angles ( $\alpha$ ) ranging from 0° to 45° with an interval of 7.5°. The illustration of the wind attack angle is shown in Fig. 4.

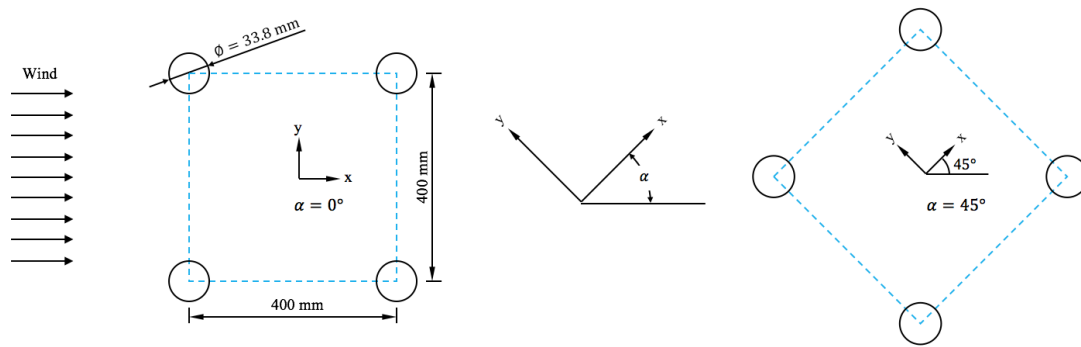


Fig. 4 Shape of the four-bundled conductor and wind attack angle in wind tunnel tests

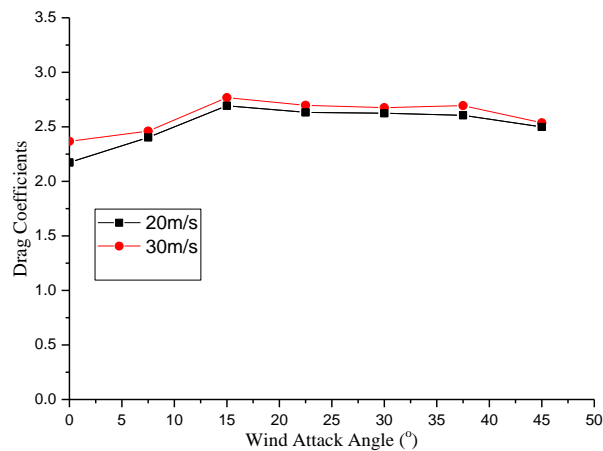


Fig. 5 Drag coefficients for four-bundled conductor

Then the drag coefficients for the four-bundled conductor are calculated in the same way as for the transmission tower. The drag forces are directly from the force balance measurements for the entire four cables. Meanwhile, it should also be noted that the projected area is calculated from one single cable instead of the entire four cables.

The tested drag coefficients of the four-bundled conductor model for each wind speed and wind attack angle are shown in Fig. 5. As shown in Fig. 5, the difference in drag coefficients between these two wind speeds are limited and the drag coefficients vary mildly with wind attack angles due to the gradually varying projected area of the four-bundled conductor. For both wind speeds, the maximum drag coefficients occur at the attack angle of 15°

## 4. Results and discussions

### 4.1 Dynamic analysis

To evaluate the dynamic performance of the entire transmission tower-line system under different situations, six groups of dynamic analyses are carried out in the time domain with three different corrosion conditions with a combination of whether or not including the aerodynamic

damping in the analysis. Based on the wind loads defined in Eqs. (1) and (2) for the transmission towers and conductors as well as the drag coefficients obtained from the wind tunnel experiments, the dynamic response of the transmission tower-line system can be obtained. For instance, Fig. 6 shows the time history of the tower top-tip displacement and the base shear force at the wind speed of 30 m/s and the wind yaw angle of 90° for the non-corrosive transmission tower model without considering the aerodynamic damping effect on the conductors. Similar to the definition of the gust wind factor used to describe a sudden increase of the wind speed, a gust response factor could also be defined as the ratio of the maximum response to the mean response based on the time history of a certain structural response parameter. As shown in Figure 6, a gust response factor of 1.285 and 1.375 can be obtained for the tower top-tip displacement and the base shear force, respectively.

Fig. 7 shows the corresponding response spectral density for the tower top-tip displacement and the base shear force. As shown in Fig. 7, the resonant response component could be distinguished from the background component. Meanwhile, the first resonant mode is centered at the frequency of 1.478 Hz and 1.463 Hz for the tower top-tip displacement and the base shear force, respectively, which match the first modal frequency of the tower.

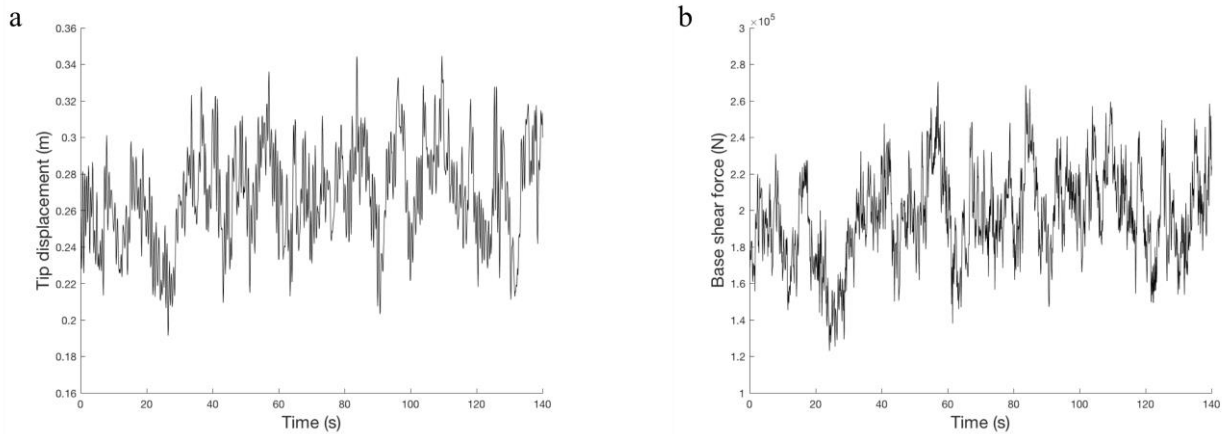


Fig. 6 Time history for: (a) top-tip displacement and (b) base shear force

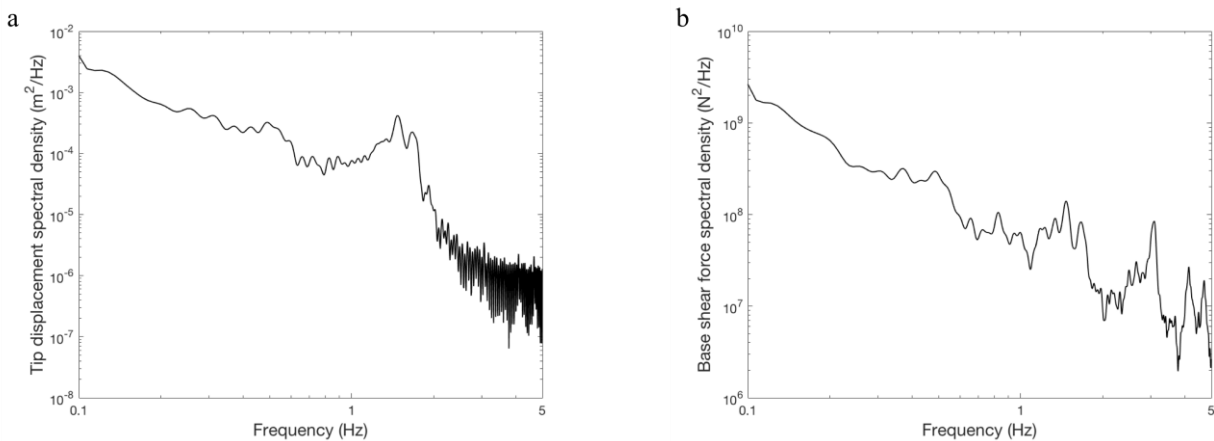


Fig. 7 Response spectral density for: (a) top-tip displacement and (b) base shear force

It should be mentioned that the dynamic analysis is carried out using an 80 s wind load time history and a ramp load of 3 s is applied at the beginning of the simulation to reduce the dynamic instability caused by the suddenly applied wind loads. To investigate whether 80 s simulation time is long enough to capture the important information from the interactions between wind and structures, a sensitivity analysis is conducted using a simulation time of 80 s and 150 s for comparison. The results indicate that the difference of the maximum values of the tower top-tip displacement is only 2.5% in these two simulations. To reduce the calculation cost in the following calculation cases, 80s are used for all the dynamic analyses in the present study.

#### 4.2 Capacity curve

The capacity curves for the transmission tower with different combinations of corrosion conditions and whether or not including the aerodynamic damping are obtained to show the relationship between the maximum top-tip displacement and the maximum base shear force. For the sake of brevity, only the relationships between the top-tip

displacement and the base shear force for the wind yaw angle of  $60^\circ$  are shown in Figs. 8 and 9 as the capacity curves. As shown in these figures, a similar post-yield behavior with small stiffness could be observed due to the nonlinear structural models considered in the present study. In addition, a small nonlinearity could be observed for some capacity curves at the beginning of the elastic range. This is due to the incremental dynamic analysis (IDA) approach used in the present study, which is based on performing dynamic analysis and obtaining damage measures (DMs) from the response time history. Since the wind loads are stochastic, uncertainty exists in the structural response and therefore results in a small nonlinearity in the elastic range of the capacity curves. The capacity curves for other three wind directions are similar. Figs. 8(a)-8(c) show the capacity curves for the transmission tower without corrosion, with slight corrosion 15 years after the construction, and with severe corrosion 25 years after the construction. In each figure, two curves are plotted corresponding to the simulation cases with or without consideration of the aerodynamic damping effect on the conductors. As shown in Fig. 8, all capacity curves exhibit a similar behavior of moving from the linear elastic range to

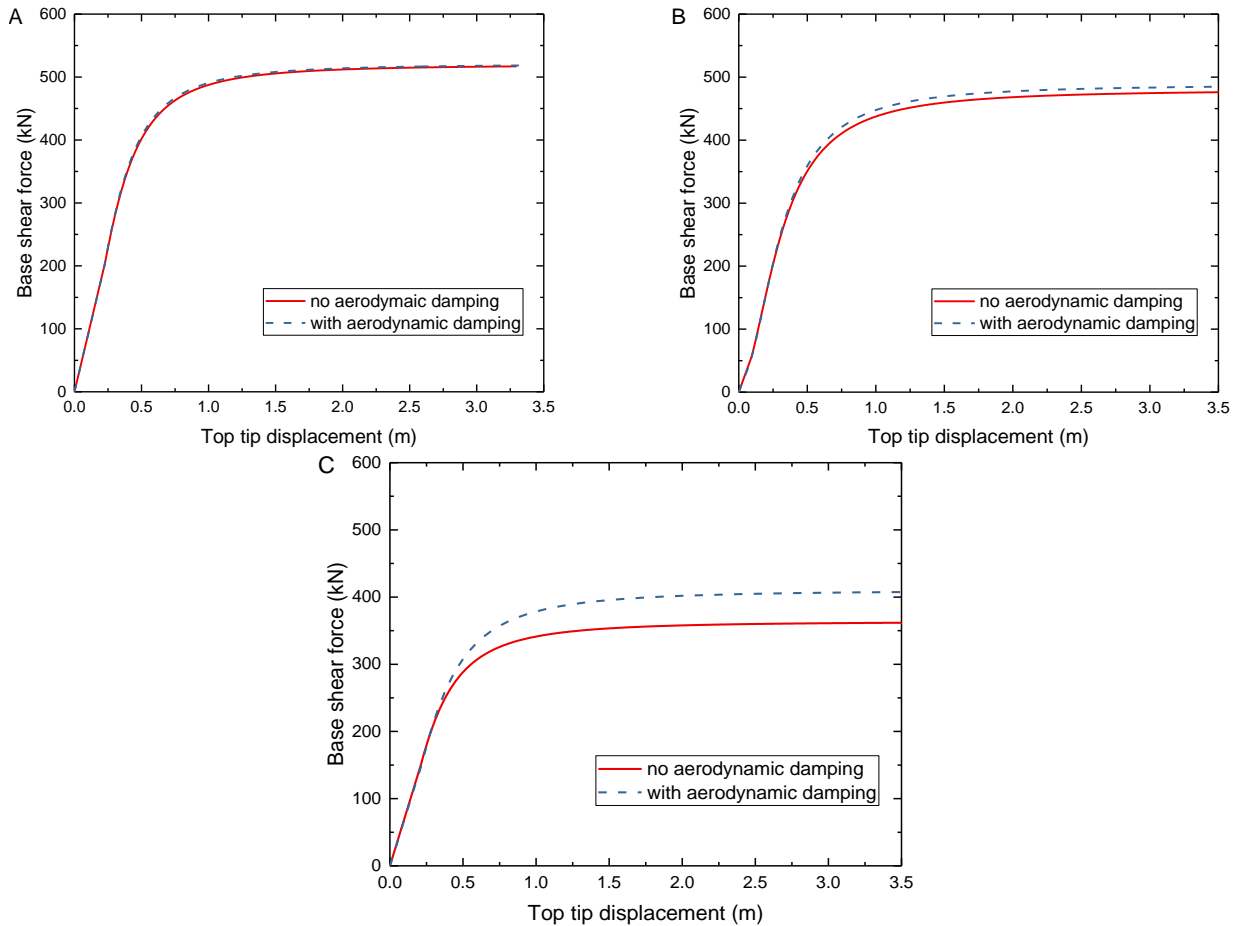


Fig. 8 Capacity curves for: (a) tower without corrosion (b) tower with slight corrosion and (c) tower with severe corrosion

the plastic range as the top-tip displacement increases. Meanwhile, only limited differences can be found for the force-displacement curves in the lower elastic range, which implies that the aerodynamic damping has little effect when the deflection of the transmission tower is small under lower wind speeds.

As shown in Fig. 8(a), the two capacity curves are almost the same in both the linear elastic range and the plastic range and the structure begins to yield when the top-tip displacement is above around 0.5 m and the base shear force is around 400 kN. Therefore, the aerodynamic damping has little effect on the elastic-plastic behavior of the transmission tower without corrosion. Fig. 8(b) shows the capacity curves for the transmission tower with slight corrosion. As shown in Fig. 8(b), the two capacity curves are only similar in the structural elastic range. When yielding begins to develop in the transmission towers, the force-displacement curves for the simulations with and without consideration of the aerodynamic damping gradually deviate from each other and remains in a parallel relationship in the plastic range. In addition, the slightly corrosive transmission tower is in an elastic range when the top-tip displacement is below around 0.4 m and the base shear force is below around 350 kN. A 2.2% difference in the base shear force at the same top-tip displacement

remains in the plastic range. Therefore, the aerodynamic damping has a minor effect on the dynamic behavior of the transmission tower with slight corrosion in the plastic range. Moving forward, as shown in Fig. 8(c), the capacity curves for the severely corrosive transmission tower show a similar trend to those observed in Fig. 8(b). However, the force-displacement curves for the simulations with and without implementing the aerodynamic damping deviate much more from each other after structure yielding and a 12.1% difference in the base shear force remains in the plastic range. Meanwhile, the transmission tower with severe corrosion begins to yield when the top-tip displacement is above around 0.35 m or 0.3 m and the base shear force is above around 300 kN or 250 kN for the simulation cases with and without consideration of the aerodynamic damping, respectively. The results suggest that the aerodynamic damping force, therefore, could play an important role in affecting the dynamic behavior of the transmission tower when the structural members begin to yield. It is also noteworthy that the aerodynamic damping force on the conductors could increase the capacity of the entire transmission tower-line system under strong wind loadings, especially when there exists corrosion penetration on the transmission tower.

Table 3 Tower natural frequencies

Tower model	1 <sup>st</sup> natural frequency (Hz)	2 <sup>nd</sup> natural frequency (Hz)
No corrosion	1.592	1.651
15 years corrosion	1.635	1.694
25 years corrosion	1.671	1.729

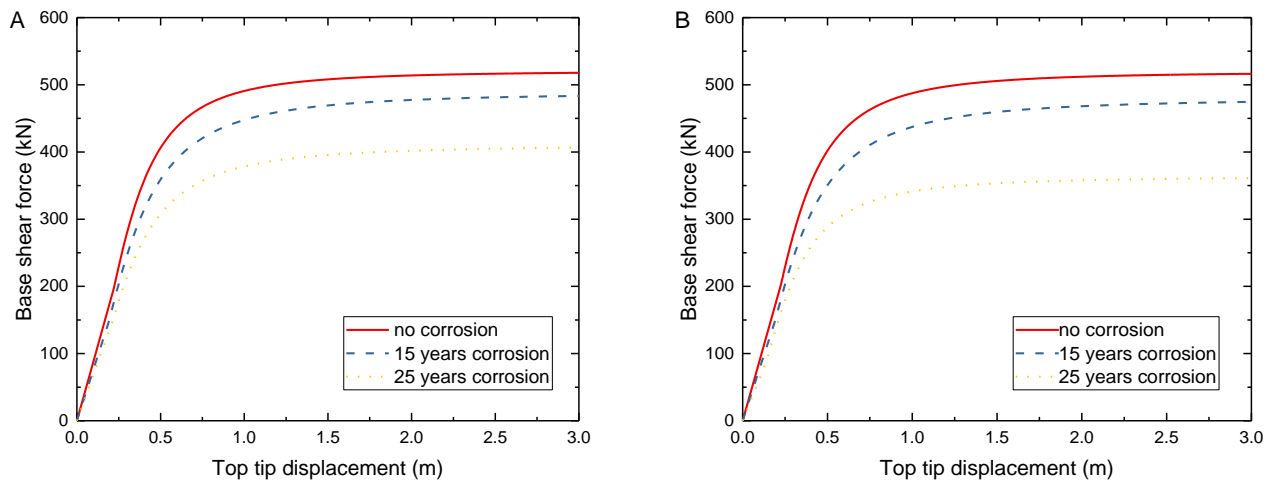


Fig. 9 Capacity curves: (a) with aerodynamic damping force on conductors and (b) without aerodynamic damping force on conductors

A further investigation on the effect of the aerodynamic damping on the corroded and non-corroded models is also conducted by comparing the natural frequencies of the three tower models. Table 3 shows the first two natural frequencies of the three tower models. As shown in Table 3, the natural frequencies of the corroded towers are slightly increased, which is a combination result of the stiffness reduction and mass loss. Since the thickness and therefore the cross-sectional area of the tower members is reduced for the corroded towers, both the stiffness and mass properties of the entire tower could be affected. In addition, the differences in the natural frequencies of these three tower models are limited, which indicates that the large effect of the aerodynamic damping on the capacity of the corroded tower might not due to the structural natural frequencies. However, a detailed study considering a corroded tower with different natural frequencies is necessary to be carried out to further address this problem.

To better illustrate the effects of the corrosions, the capacity curves for the transmission tower with and without consideration of the aerodynamic damping effect are also shown in Figs. 9(a) and 9(b) and each figure consists of three curves representing different corrosion conditions of the transmission tower. After considering the aerodynamic damping, as shown in Fig. 9(a), the corrosion could affect the dynamic behavior of the transmission tower in the higher elastic range when the transmission tower-line system is subjected to a higher wind speed. Meanwhile, the yield strength of the transmission tower could also be substantially affected by the corrosion penetration on the transmission tower. A 7.6% and 22.1% difference in the yield strength could be found, respectively, between the

tower without corrosion and with slight corrosion and between the tower without corrosion and with severe corrosion. Therefore, the corrosion penetration on the transmission tower could significantly decrease the capacity of the transmission tower-line system. Same conclusion could be drawn for the simulation cases without consideration of the aerodynamic damping as shown in Fig. 9(b). The difference in the yield strength is 9.1% between the non-corrosive tower and the slightly corrosive tower and is 30.1% between the non-corrosive tower and the severely corrosive tower. Regarding to the difference in yield strength, the capacity of the transmission tower-line system tends to have more variation when not applying the aerodynamic damping force on the conductors. Therefore, it is necessary to evaluate the corrosion condition of the existing transmission tower with a more accurate modeling and updating scheme to assess their structural capacity.

#### 4.3 Extreme value analysis

To further evaluate the effect of the corrosion on the extreme response of the transmission tower-line system, extreme value analysis is carried out using the time history of the tower top tip displacement and base shear force. All the local maxima, which are defined as the maximum value between two successive zero up-crossing mean values, are extracted first from the time history of the responses. To exclude the small values in the local maximum values, some threshold values can be defined. However, selection of the threshold value is empirical and could affect the results. The distribution types and associated descriptors of the peak values could change, as well, from a practical

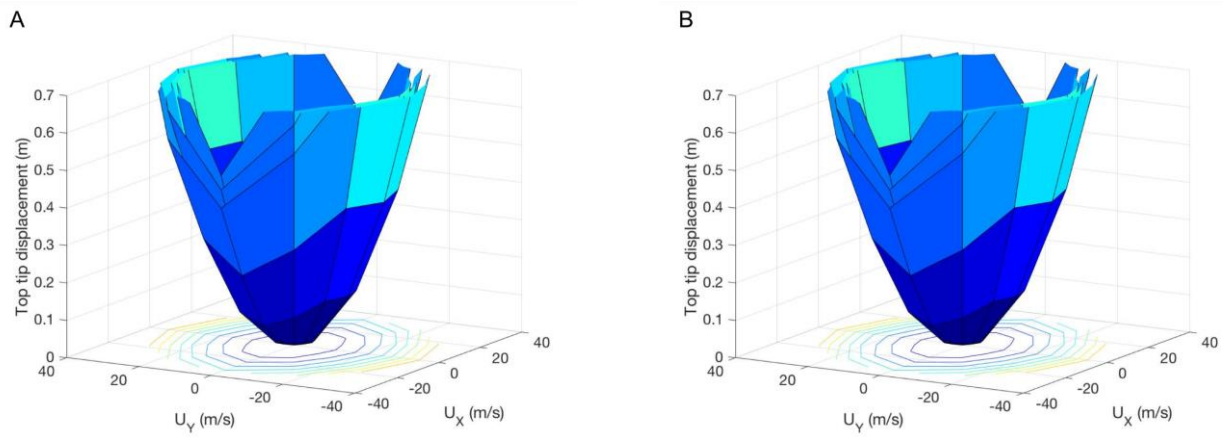


Fig. 10 Extreme value surface for top-tip displacement: (a) with aerodynamic damping effect and (b) without aerodynamic damping effect

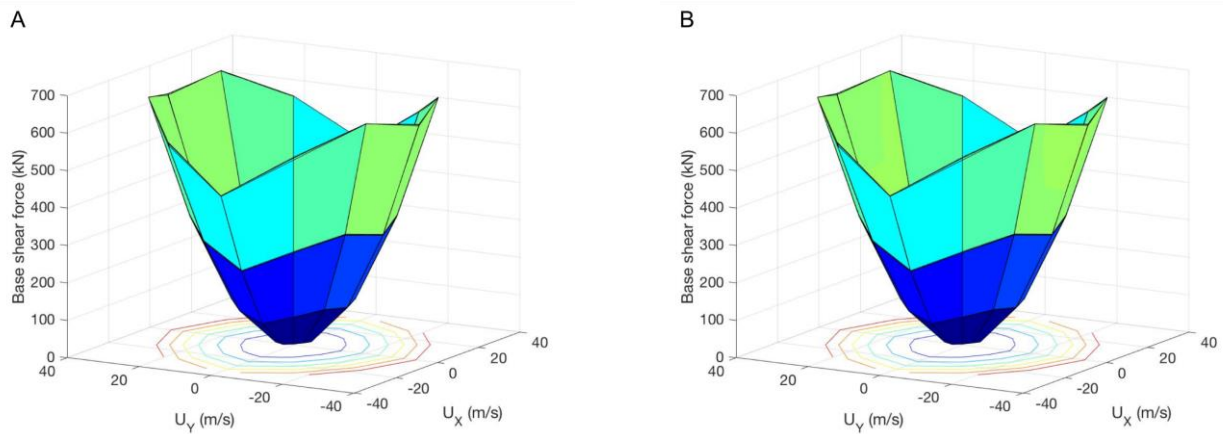


Fig. 11 Extreme value surface for base shear force: (a) with aerodynamic damping effect and (b) without aerodynamic damping effect

viewpoint. In the present study, the threshold value is defined as the mean value of the response plus 1.4 times the standard deviation of the response (Moriarty *et al.* 2004). After obtaining the peaks above this threshold, Weibull distribution can be used to fit the peak values based on the extreme value analysis theory (Kotz and Nadarajah 2000). Meanwhile, for the design purpose, one might be interested in the short-term extreme response corresponding to one particular wind direction and wind speed. Since the average wind speeds are usually reported based on 10 minutes to represent a stationary wind condition, the short-term extreme response is evaluated according to 10-minutes duration in the present study. The extreme response can then be estimated based on the Weibull distribution of the peaks and the time duration of the stationary response of the transmission tower-line system using the following equation

$$F_T(y) = [F_S(x)]^{\nu_S T} \quad (8)$$

where  $S = 60$  sec is the simulation time used for extracting the peaks;  $T = 10$  min is the time duration of the short-term

response;  $F_T(y)$  is the cumulative distribution function of the extreme value;  $F_S(x)$  is the cumulative distribution function obtained by fitting the Weibull distribution to the peaks; and  $\nu_S$  is the mean occurring frequency of the peaks and is calculated as  $\nu_S = N/S$ , where  $N$  is the total number of peaks in each simulation. After obtaining  $F_T(y)$ , various statistical properties of the extreme values could be evaluated. In this study, the probable extreme value,  $Y_P$ , defined as the extreme value most likely to occur in the short-term response, is adopted to evaluate the extreme response of the transmission tower-line system at different wind directions and wind speeds and is calculated as (Ochi 1981)

$$Y_P = \sqrt{2 \ln \left( \frac{60^2 T}{2\pi} \sqrt{\frac{m_2}{m_0}} \right)} \sqrt{m_0} \quad (9)$$

where  $T$  is time in hours, which is  $10/60$  in the present study;  $m_0$  is the area under the response spectrum; and  $m_2$  is the second moment of the response spectrum.

Based on the extreme value analysis, the extreme response of the tower top-tip displacement for the simulation cases of whether or not including the aerodynamic damping effect at all wind directions and wind speeds are shown in Figs. 10(a) and 10(b), respectively. In both figures, the bottom surface corresponds to the simulations with non-corrosive tower, the middle surface corresponds to the simulations with slightly corrosive tower, and the top surface corresponds to the simulations with severely corrosive tower. Based on Fig. 10, the extreme response surface of the tower top-tip displacement for the towers with more severe corrosion provides an approximate upper bound to the extreme response surface for the towers with less corrosion. Meanwhile, the tower top-tip displacement increases at a faster rate as the wind direction becomes increasingly perpendicular to the conductors. Figs. 11(a) and 11(b) show the extreme response of the tower base shear force for the simulations with and without consideration of the aerodynamic damping effect. As shown in Fig. 11, the extreme response surfaces of the tower base shear force for towers with different corrosion conditions only have small differences. Therefore, the extreme value of the tower base shear force is not sensitive to the corrosion condition of the transmission tower. Similarly, the extreme value of the tower base shear force increases at a faster rate when the wind direction is perpendicular to the conductors.

## 5. Conclusions

In the present study, the dynamic response of the transmission tower-line system is evaluated considering different corrosion conditions of the transmission tower as well as the effect from the aerodynamic damping force on the conductors. Corrosion on the connections is not considered in the present study. Sensitivity analysis is carried out based on the incremental dynamic analysis (IDA) to evaluate the dynamic performance of the tower-line system and capacity curves are obtained. In addition, extreme value analysis is also performed to estimate the extreme response of the tower top-tip displacement and the base shear force based on the peak values fitting method.

From the present study, the following conclusions are drawn: (1) the corrosion penetration on the transmission towers could significantly decrease the capacity of the transmission tower-line system under strong winds; (2) the aerodynamic damping force on the conductors could increase the capacity of the transmission tower-line system under strong wind loadings, especially when there exists corrosion penetration on the transmission tower; (3) With the inclusion of corrosion, the tower top-tip displacement is larger than the cases without inclusion of corrosion based on the short-term extreme analysis. Therefore, it is necessary to include the corrosion condition of the transmission towers for the capacity analysis of existing transmission tower-line system, which could rely on more advanced contacting or non-contact sensing technologies and advanced data process schemes. In addition, corrosion effects on connections, which are not included in the present study, should be carefully studied, as well.

## Acknowledgments

This material is based upon work supported by the National Science Foundation of China under Grant Number 51478181, U1534206, China Scholarship Council (No. 201506135039), and Bentley Systems. The support is greatly appreciated. Any opinions, findings, and conclusions or recommendations expressed in this material are those of the authors and do not necessarily reflect the views of the sponsors.

## References

- Aboshosha, H. and El Damatty, A. (2015), "Engineering method for estimating the reactions of transmission line conductors under downburst winds", *Eng. Struct.*, **99**, 272-284.
- Aboshosha, H., Elawady, A., El Ansary, A. and El Damatty, A. (2016), "Review on dynamic and quasi-static buffeting response of transmission lines under synoptic and non-synoptic winds", *Eng. Struct.*, **112**, 23-46.
- Albrecht, P. and Naeemi, A.H. (1984), "Performance of weathering steel in bridges", *NCHRP Report 272*, Washington.
- Banik, S., Hong, H. and Kopp, G.A. (2008), "Assessment of structural capacity of an overhead power transmission line tower under wind loading", *BBAA VI International Colloquium on Bluff Bodies Aerodynamics & Applications*, 20-24.
- Banik, S.S., Hong, H.P. and Kopp, G.A. (2010), "Assessment of capacity curves for transmission line towers under wind loading", *Wind Struct.*, **13**(1), 1-20.
- Chen, X. (2013), "Estimation of stochastic crosswind response of wind-excited tall buildings with nonlinear aerodynamic damping", *Eng. Struct.*, **56**, 766-778.
- Czarnecki, A.A. and Nowak, A.S. (2008), "Time-variant reliability profiles for steel girder bridges", *Struct. Saf.*, **30**(1), 49-64.
- Darwish, M. and El Damatty, A. (2017), "Critical parameters and configurations affecting the analysis and design of guyed transmission towers under downburst loading", *Practice Periodical Struct. Des. Constr.*, **22**(1), 4016017.
- Deng, H.Z., Xu, H.J., Duan, C.Y., Jin, X.H. and Wang, Z.H. (2016), "Experimental and numerical study on the responses of a transmission tower to skew incident winds", *J. Wind Eng. Ind. Aerod.*, **157**, 171-188.
- Deodatis, G. (1996), "Simulation of ergodic multivariate stochastic processes", *J. Eng. Mech.*, **122**(8), 778-787.
- Dua, A., Clobes, M., Höbbel, T. and Matsagar, V. (2015), "Dynamic analysis of overhead transmission lines under turbulent wind loading", 15(December), 359-371.
- Elawady, A., Aboshosha, H., El Damatty, A., Bitsuamlak, G., Hangan, H. and Elatar, A. (2017), "Aero-elastic testing of multi-spanned transmission line subjected to downbursts", *J. Wind Eng. Ind. Aerod.*, **169**, 194-216.
- Elawady, A. and El Damatty, A. (2016), "Longitudinal force on transmission towers due to non-symmetric downburst conductor loads", *Eng. Struct.*, **127**, 206-226.
- Hamada, A., King, J.P.C., El Damatty, A.A., Bitsuamlak, G. and Hamada, M. (2017), "The response of a guyed transmission line system to boundary layer wind", *Eng. Struct.*, **139**, 135-152.
- Jacobs, M. (2013), "13 of the Largest Power Outages in History — and What They Tell Us About the 2003 Northeast Blackout", *Union of Concerned Scientists, Science for a healthy planet and safer world*, (August 8).
- Kaimal, J.C., Wyngaard, J.C., Izumi, Y. and Coté, O.R. (1972), "Spectral characteristics of surface-layer turbulence", *Q. J. Roy. Meteor. Soc.*, **98**(417), 563-589.
- Keyhan, H., McClure, G. and Habashi, W.G. (2013), "Dynamic

- analysis of an overhead transmission line subject to gusty wind loading predicted by wind-conductor interaction”, *Comput. Struct.*, **122**, 135-144.
- Komp, M.E. (1987), “Atmospheric corrosion rating of weathering steel”, *Calculations and significance*.
- Kotz, S. and Nadarajah, S. (2000), *Extreme value distributions*. Imperial College Press, London.
- Lee, K.M., Cho, H.N. and Cha, C.J. (2006), *Life-cycle cost-effective optimum design of steel bridges considering environmental stressors*, *Engineering Structures*.
- Liang, S., Zou, L., Wang, D. and Cao, H. (2015), “Investigation on wind tunnel tests of a full aeroelastic model of electrical transmission tower-line system”, *Eng. Struct.*, **85**, 63-72.
- Lin, W.E., Savory, E., McIntyre, R.P., Vandelaar, C.S. and King, J. P.C. (2012), “The response of an overhead electrical power transmission line to two types of wind forcing”, *J. Wind Eng. Ind. Aerod.*, **100**(1), 58-69.
- Mara, T.G. (2013), “Capacity assessment of a transmission tower under wind loading”.
- Mara, T.G. and Hong, H.P. (2013), “Effect of wind direction on the response and capacity surface of a transmission tower”, *Eng. Struct.*, **57**, 493-501.
- Meehl, G. A., Zwiers, F., Evans, J., Knutson, T., Mearns, L. and Whetton, P. (2000), “Trends in extreme weather and climate events: issues related to modeling extremes in projections of future climate change”, *Bull. Am. Meteorol. Soc.*, **81**(3), 427-436.
- Moriarty, P.J., Holley, W.E. and Butterfield, S.P. (2004), “Extrapolation of extreme and fatigue loads using probabilistic methods”, *National Renewable Energy Laboratory*, (November), 500-34421.
- Nowak, A.S. and Thoft-Christensen, P. (2000), “International Contribution to the Highways Agency’s Bridge Related Research”, *Bridge Rehabilitation in the UK: Review of the Current Programme and Preparing for the Next*.
- Nowak, A. and Szerszen, M. (2001), “Reliability profiles for steel girder bridges with regard to corrosion and fatigue”, *J. Theor. Appl. Mech.*, **39**(2), 339-352.
- Ochi, M. (1981), “Principles of extreme value statistics and their application”, *Extreme Loads Response Symposium*, 15-30.
- De Oliveira, A., Silva, E., De Medeiros, J.C.P., Loredou-Souza, A. M., Rocha, M.M., Rippel, L.I., Carpeggiani, E.A. and Núñez, G. J.Z. (2006), “Wind loads on metallic latticed transmission line towers”, *Proceedings CIGRE Session 2006*.
- Park, C.H. and Nowak, A.S. (1997). “Lifetime reliability model for steel girder bridges”, *P.C. Das (Ed.), Safety of bridges*, Thomas Telford Publishing, London.
- Stengel, D. and Mehdianpour, M. (2014), “Finite element modelling of electrical overhead line cables under turbulent wind load”, *J. Struct.*, 1-8.
- Takeuchi, M., Maeda, J. and Ishida, N. (2010), “Aerodynamic damping properties of two transmission towers estimated by combining several identification methods”, *J. Wind Eng. Ind. Aerod.*, **98**(12), 872-880.
- Yang, S.C. and Hong, H.P. (2016), “Nonlinear inelastic responses of transmission tower-line system under downburst wind”, *Eng. Struct.*, **123**, 490-500.
- Yuan, H., Zhang, W., Zhu, J. and Bagtzoglou, A. (2017), “Structural Reliability assessment of a single-circuit overhead distribution system under extreme wind hazard”, *Proceedings of the 13<sup>th</sup> Americas Conference on Wind Engineering*, May 21-24, 2017, Gainesville, FL.
- Zhang, W., Zhu, J., Liu, H. and Niu, H. (2015), “Probabilistic capacity assessment of lattice transmission towers under strong wind”, *Frontiers in Built Environ.*, **1**, 1-12.

AD